

## Modeling and estimation of evapotranspiration using remote sensing and GIS technologies in some areas of southern Iraq

Dakhil. R. Nedawi<sup>1</sup> , Forqan Kh. Al-Draji<sup>2</sup>

Soil and Water Resources Sciences- College of Agriculture - University of Basrah - Basrah – Iraq<sup>1</sup> , Energy, Environment and Water Unit - Presidency of Basrah University - Basrah – Iraq<sup>2</sup>

Received on 1/05/2022 Accepted on 26/06/2022 Published on 30/06/2022

### Abstract

A study was conducted in southern Iraq. The study area was 16485.4418 km<sup>2</sup> with the administrative boundaries of Basrah (North region) and Dhi-Qar (south region) Governorates. The aim of this study to design a digital model for estimating evapotranspiration values (mm) using remote sensing data and geographic information systems and comparing the results with the actual values calculated from four climatic stations distributed within the study area. As well as to study January and July from each year for a four-years chronology. The results showed that there is a highly significant correlation ( $r = 0.923^{**}$ ) between the calculated and actual values, and this proves the accuracy of the proposed model in estimating the values of evapotranspiration. The results also showed that there is a rise in the values of evapotranspiration in the month of July compared to the month of January of each year due to the high temperatures and the angle of incidence of the sun's rays, which is almost vertical in the month of July. The results also showed that the study area varies in the values of evapotranspiration according to the different vegetation cover, as the values decrease with the increase of vegetation cover and Vice versa. As well as the effect of the values of evapotranspiration by rising for limited areas in the areas of electric power plants and oil fields, and this gives evidence of large quantities of thermal and radioactive emissions in the areas. The results also showed that there is a inconsistency between the values of evapotranspiration and the areas covered, which were divided into four categories for each scene, and that the values of these categories differ according to the types of land cover.

**Key words:** : Evapotranspiration modeling, Remote sensing, GIS, Soil temperature,

### Introduction

The change in the values of evapotranspiration is an important indicator of the water balance cycle

equation directly affects the management of water resources, which requires an accurate estimation of this factor for large

areas and for multiple periods of time in arid and semi-arid areas, especially in southern Iraq (Hamed, 2019). It is necessary to design simulation models or empirical equations using modern techniques to obtain data instead of traditional methods for estimating evapotranspiration, such as weather stations that cover relatively limited areas compared to satellite image, and at the lowest costs or the need for labor force (Onwuka and Mang, 2018). The progress in the use of remote sensing and geographic information systems (GIS), especially in the agricultural fields, that can be used to estimate evapotranspiration in large areas, as it is possible to obtain one reading for each area unit (900 m<sup>2</sup>) if the pixel dimensions are 30 \* 30 m, which are the image, freely available for the Landsat 8 satellite (González et al., 2018). Modern methods for calculating evapotranspiration depend on heat balance models, electromagnetic energy and types of land cover, especially vegetation, which is an effective factor in the process of evapotranspiration. Therefore, digital data can be modeled and equations can be derived from them and mathematical formulas that help estimate evapotranspiration according to the scientific bases of evapotranspiration remote sensing. After that it can be applied on the agricultural fields and compared with field methods or for large areas such as climatic stations data (Gontia and Tiwari, 2010). Then calculating the correlation coefficient between the values drawn by modeling and the common field values of climatic stations data.

This aim of this study was to use remote sensing technologies and GIS systems in modeling and estimating evapotranspiration in some areas of southern Iraq.

#### **Office work and methods**

The study was conducted on an area of about 16,485.4418 km<sup>2</sup> located within the borders of Basra and Dhi-Qar governorates southern cities of Iraq. The area covers Chibayish Marshes (Southeast of Dhi-Qar Governorate) and adjacent lands in center and north of Basrah Governorate.

#### **Field work**

Field data for evapotranspiration values were collected from four climatic stations including two stations in Basra (Al-Qurna, Al-Burjisya) and two in Dhi Qar (Al-Jabaish, Sugalsheyowkh) for two months January and July for four years (2019, 2018, 2021 and 2020).

#### **Office work:**

Satellite images of Landsat 8 satellite were downloaded from the USGS website to four years for each January and July months, according to each row and path to satellite, which gives a snapshot covering study area. Digital data for fourth, fifth and tenth spectral bands were processed and evapotranspiration values were calculated using following steps (Howari et al. , 2006):

**1- The vegetation cover index was calculated using each image according to equation No. (1).**

$$NDVI = \frac{B5 - B4}{B5 + B4} \dots \dots (1)$$

**NDVI: Vegetation index that ranges (from 1 to -1).**

**B4: Fourth spectral band of red rays.**

**B5: Fifth spectral band of near infrared rays.**

**2- The vegetation coverage areas (portion of vegetation)) was calculated using equation No. (2).**

$$PV = ((NDVI - NDVI \text{ min}) / (NDVI \text{ max} - NDVI \text{ min}))^2 \dots \dots (2)$$

**PV: vegetative coverage.**

**NDVI: Vegetation Index for Satellite Image.**

NDVI max/min: lower and higher value of vegetation index than image.

- 3- The Land Surface Emissivity was calculated using Equation No. (3).

$$E = 0.004 * PV + 0.986 \dots \dots (3)$$

PV: vegetative coverage.

- 4- The radiation in upper atmosphere (TOA) was calculated using equation No. (4) (Hamed, 2019)

$$L(\lambda) = ML * \text{Band } 10 + AL - O_i \dots \dots (4)$$

$L(\lambda)$  : spectral radiance (TOA).

ML&AL: Constants for tenth spectral band and can be obtained from the file attached with the satellite image.

$O_i$ : correction factor for the tenth spectral band (0.29).

Band 10 : The tenth thermal spectral band.

- 5- The radiation temperature at the top of the atmosphere from Kelvin to Celsius was converted using Equation No. (5).

$$BT = (1321.0789 / \ln(774.885 / \text{"TOA"} + 1)) - 273.15 \dots \dots (5)$$

$L(\lambda)$ : spectral radiance TOA).

BT: The temperature of the radiation above the atmosphere in Celsius.

K2&K11: Constants for the tenth package of the file attached with satellite image.

- 6- The Earth's temperature (LST) was calculated using equation No. (6) (Lal and Shukla, 2004):

$$LST = BT / (1 + (\lambda * BT / C2) * \ln(E)) \dots \dots (6)$$

LST: Earth's surface temperature in Celsius.

BT: Temperature of radiation above the atmosphere in Celsius.

E: Thermal emissivity of Earth's surface.

- 7- The evapotranspiration vales were calculated using equation No. (7) mentioned in (Howari et al., 2022):  
 $ET_o = 0.66 + 0.052 * (LST) + 1.37 * (NDVI) \dots \dots (7)$

ET<sub>o</sub>: Value of evapotranspiration in mm .

- 8- Calculating of evapotranspiration equation was modified according to Iraqi climatic conditions, which was depended on relied upon and which represents the model used in data modeling (Equation No. 8):

$$ET_{oED} = 0.819 + 0.8202 * (ET_o \text{ From satellite image}) \dots \dots (8)$$

ET<sub>oED</sub>: The modified evapotranspiration value in mm that represents the actual evapotranspiration in the areas southern of Iraq.

- 9- According to the correlation coefficient using SPSS program, which was amounted to  $r = 0.923^{**}$  between values of four climatic stations with the values that were estimated using digital modeling of locations of same climatic stations for four years and for January and July months of each year and according to date of capturing the space scene.
- 10- The study area was divided in each month into four categories according to the values of evapotranspiration and date of capturing same space scene. Area of each category was also calculated and its percentage from the total area.

## Results and discussion:

### Correlation between field values and numeric model values

Table 1 and Figure 1 showed direct field evapotranspiration values from climatic stations and evapotranspiration values using numerical modeling and the correlation between them. The a correlation value was  $r = 0.923^{**}$  between the measured and field values, and this indicates the possibility of adopting this

model in estimating evapotranspiration instead of the traditional field methods that require costs, time and effort, as well as covering relatively limited areas. The digital model depends on calculating the amount of solar radiation, air temperature and the surface of the earth, as well as the

vegetation cover variation, which has a significant impact on the value of evapotranspiration in the studied area. This gives a good priority to remote sensing and GIS in estimating the factors on which the evapotranspiration calculation depends (Howari et al., 2022).

**Table (1): Field evapotranspiration values from weather stations and values were obtained using digital modeling of satellite image.**

Evapotranspiration values from climate stations (mm)	Evapotranspiration values from satellite image (mm)	Date	station
2.40	2.41	1/15/2018	1
12.40	11.40	7/26/2018	1
2.10	1.95	1/18/2019	1
9.60	9.10	7/13/2019	1
2.00	1.73	1/15/2020	1
12.10	10.96	7/15/2020	1
3.40	2.62	1/18/2021	1
7.90	7.99	7/18/2021	1
1.97	2.40	1/15/2018	2
7.24	12.55	7/26/2018	2
1.40	2.37	1/18/2019	2
8.10	9.85	7/13/2019	2
1.85	1.92	1/15/2020	2
11.90	9.92	7/15/2020	2
2.65	2.35	1/18/2021	2
7.95	8.32	7/18/2021	2
2.50	2.22	1/15/2018	3
15.50	11.89	7/26/2018	3
2.30	2.66	1/18/2019	3
11.90	9.62	7/13/2019	3
2.20	1.85	1/15/2020	3
10.70	11.86	7/15/2020	3
2.30	3.14	1/18/2021	3
6.70	8.22	7/18/2021	3
3.50	2.19	1/15/2018	4
12.40	11.47	7/26/2018	4
2.90	2.15	1/18/2019	4
15.80	9.73	7/13/2019	4
2.50	1.95	1/15/2020	4
12.90	12.40	7/15/2020	4
2.40	2.47	1/18/2021	4
10.30	8.25	7/18/2021	4
<b>Correlation coefficient <math>r = 0.923^{**}</math> between values of four climatic stations and values that were estimated using digital modeling of locations</b>			

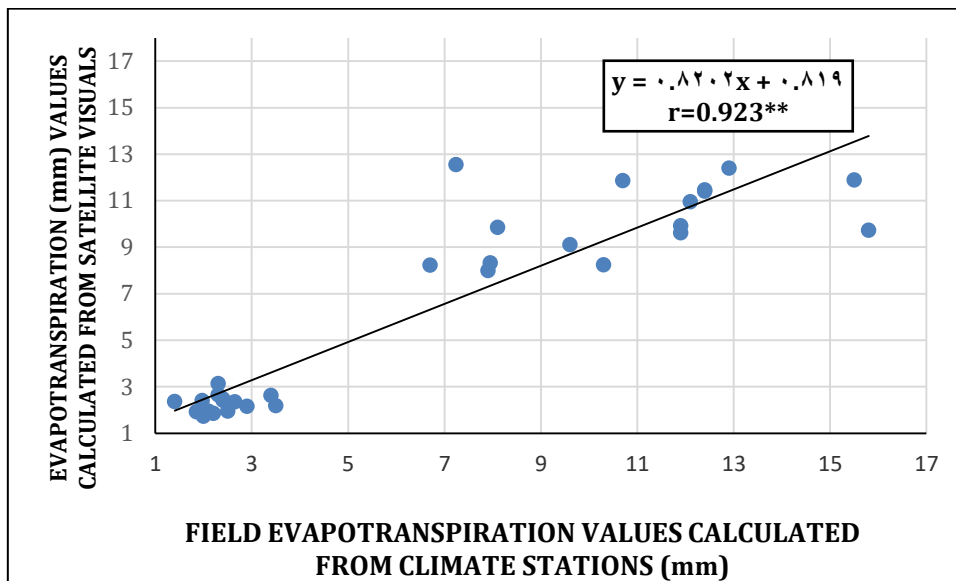


**Figure (1):** The correlation between field evapotranspiration values were calculated from weather stations and values were calculated using digital modeling of satellite image (mm).

### Evapotranspiration in study area

The results in Figure 2 and Table. 2 showed that the average values of evapotranspiration (mm) for the year of 2018, as it was found that the highest value was 19.7053 mm and the lowest value was 1,5006 mm for an area covering 0.0062% and 0.0079% of the total area, with the highest and lowest values on respectively. While most of the evapotranspiration values were ranged between the highest and lowest values and for varying areas, as the highest area percentage was 46.9454% and 78.7381% and the average values for

evapotranspiration were 2.0537 mm and 12.7860 mm in the two months of December and July, respectively. Evapotranspiration in July was compared to the evapotranspiration in January to know the effect of incoming solar rays at the top of the atmosphere, which is related to the angle of incidence as the more angle of incidence is vertical, as the greater the intensity of the incoming solar radiation. Thus, its effect increases as the evapotranspiration rates increase. The sun's rays in July are often vertical or semi vertical compared to January (Moorhead et al., 2017).

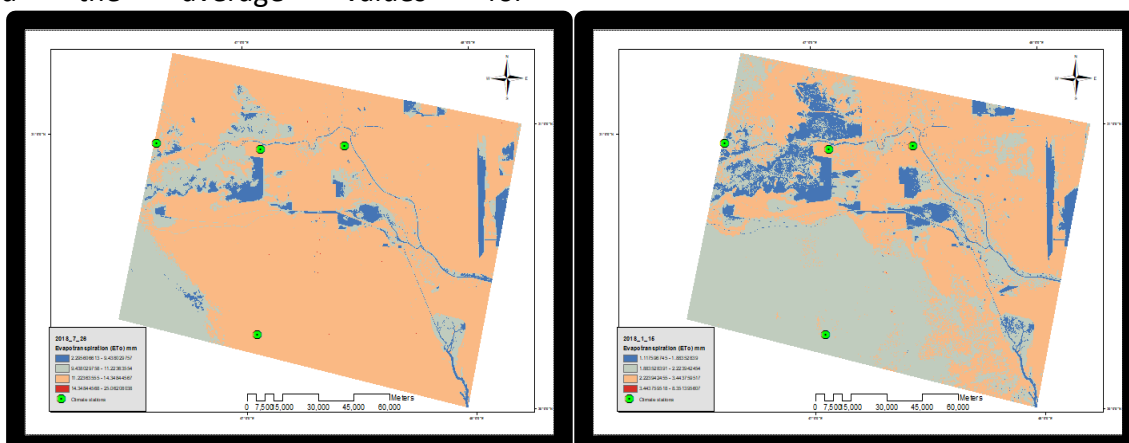


**Figure 2: A map showing the values of evapotranspiration (ETo) mm in January and July of 2018.**

Figure No. 3 and Table No. 2 show the average values of evapotranspiration (mm) for the year of 2019, as the highest values were 15.0021 mm and the lowest values were reached to 1.0086 mm for an area covering 0.0092% and 4.6219% of the total area for the highest and lowest value, respectively. While the most values of evapotranspiration were ranged between the highest and lowest values for different areas as the highest area percentage was 42.4509% and 75.6696% and the average values for evapotranspiration were 1.8850 and 9.7961 mm in January and July respectively, the reason for the different values of evapotranspiration in the study

area may be attributed to four categories and for each of the first seven months to the reflectivity coefficient and the surface-reflected short-ray energy, and according to the reflective surface, where the absorption of rays increases in paved roads, residential areas and smooth surfaces, and this leads to an increase in latent temperatures that lead to this leads to high rates of water evaporation, while short electromagnetic waves are reflected by different values from the soil according to its physical and chemical properties and vegetation cover, and thus gives different values of evaporation according to the change in the land covers (Farina, 2012).

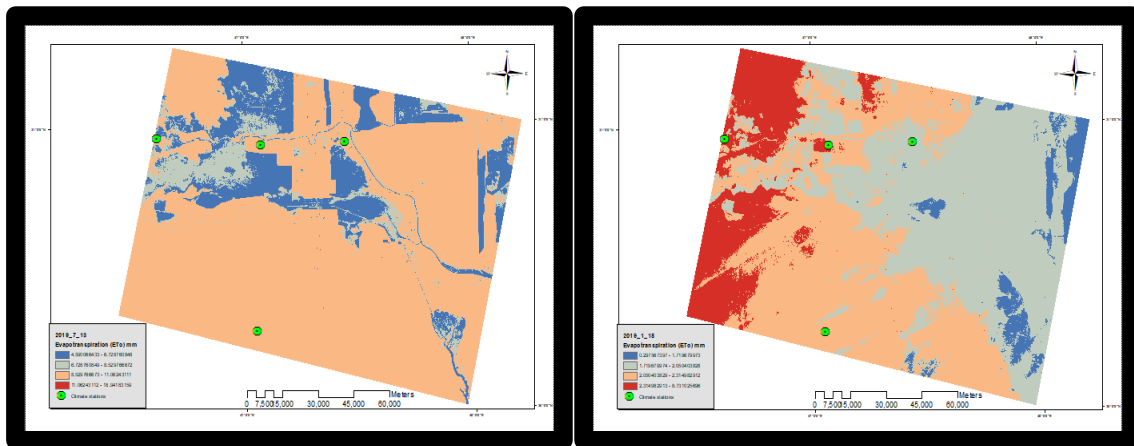


**Figure 3: A map Showing the values of evapotranspiration (ETo) mm in January and July of 2019.**

For the year of 2020, the average values of evapotranspiration as shown in Figure No. 4 and Table No. 2 were ranged between 17.1586 mm and 1.3081 mm and for an area covering percentage was 55.2370% and 18.0072% of the total area to the highest and lowest values, respectively. While most of the evapotranspiration values from transpiration were ranged between the highest and lowest values and for varying large areas and the highest spatial

coverage rate was 60.6822% and 55.2370%. The average values of evapotranspiration were recorded at 1.9192 and 17.1586 mm in the months of December and July, respectively. The reason for the variation in evapotranspiration values in the study area may be attributed to the flux of soil heat as the energy acquired by the soil or the amount of heat that leads to its heating helps to increase the rates of water evaporation and the high heating of

the soil surface leads to increasing the energy of the water inside the soil pedon in the form of moisture and thus liberating

it to the surface (Onwuka and Mang, 2018).

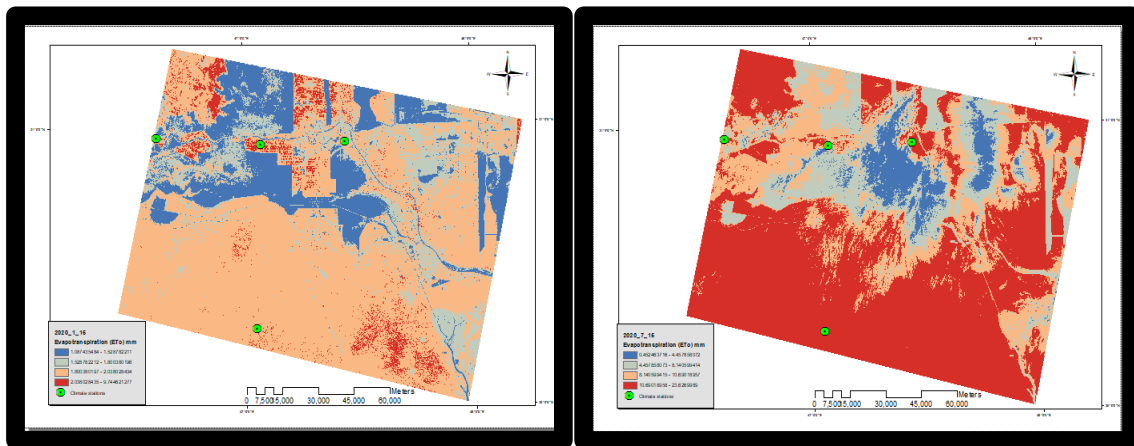


**Figure (4): A map showing the values of evapotranspiration (ETo) mm in January and July of 2020.**

For the year 2021, the results in Figure 5 and Table 2 show the average values of evapotranspiration that were ranged between 12.3034 mm and 0.6802 mm for an area covering 0.0074% and 8.8314% from the total area for the highest and lowest value, respectively. While most of the evapotranspiration values were ranged between the highest and lowest value for different areas and the highest area percentage was 38.2902 % and 53.4601% with average values of evapotranspiration of 2.7213 and 8.8444 mm in January and July, respectively. The reason for the variation in the values of evapotranspiration and for the decreasing in the areas adjacent to rivers, irrigation

channels, and some areas of the marshes is due to the increase in the density of vegetation cover in these areas, which in turn works to block the sun's rays reaching the surface of the soil and thus the decrease in soil temperature, which leads to a decrease in the value of evapotranspiration, in addition to the fact that the cultivated plants improve the properties of the soil, especially the hydraulic properties, in other words increasing the moisture content of the soil. It is known that soil moisture works to cool the microclimate and conditions, which reduces rate evapotranspiration (Howari et al. , 2022).

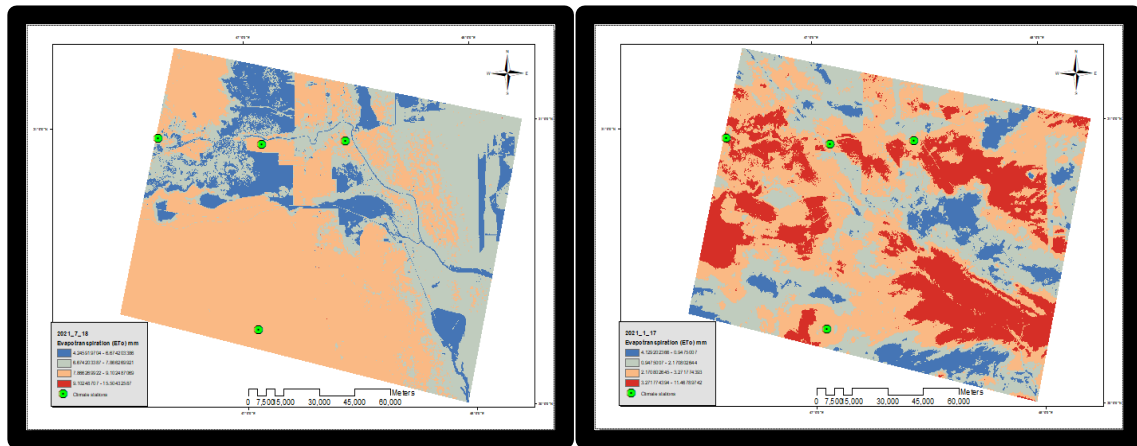


Figure (5): A map showing the values of evapotranspiration (ETo) mm in January and July of 2021 .

Table (2): Categories of evapotranspiration values (mm) in the study area, the area of each category (km<sup>2</sup>), and the percentage (%) of the area of each category of total area.

Percentage of the total area (%)	Area class (km <sup>2</sup> )	Evapotranspiration values (mm)			class	Date
		Average	Minimum	Maximum		
9.5699	1577.6411	1.5006	1.1176	1.8835	Class1	2018_1_15
46.9454	7739.1568	2.0537	1.8835	2.2239	Class2	
43.4785	7167.6162	2.8339	2.2239	3.4438	Class3	
0.0062	1.0279	5.8976	3.4438	8.3514	Class4	
4.7395	781.3226	5.8668	2.2956	9.4380	Class1	2018_7_26
16.5145	2722.4861	10.3308	9.4380	11.2236	Class2	
78.7381	12980.3299	12.7860	11.2236	14.3484	Class3	
0.0079	1.3032	19.7053	14.3484	25.0621	Class4	
4.6219	761.9439	1.0086	0.2976	1.7197	Class1	2019_1_18
42.4509	6998.2188	1.8850	1.7197	2.0504	Class2	
38.9233	6416.6730	2.1827	2.0504	2.3150	Class3	
14.0039	2308.6061	5.5230	2.3150	8.7310	Class4	
15.8875	2619.1186	5.6594	4.5901	6.7288	Class1	2019_7_13
8.4338	1390.3418	7.6293	6.7288	8.5298	Class2	

75.6696	12474.4605	9.7961	8.5298	11.0624	Class3		
0.0092	1.5209	15.0021	11.0624	18.9418	Class4		
18.0072	2968.5587	1.3081	1.0874	1.5288	Class1		2020_1_15
17.0433	2809.6635	1.6646	1.5288	1.8004	Class2		
60.6822	10003.7225	1.9192	1.8004	2.0380	Class3		
4.2674	703.4973	5.8913	2.0380	9.7446	Class4		
6.0323	994.4528	2.4552	0.4525	4.4579	Class1	2020_7_15	
16.8941	2785.0718	6.2992	4.4579	8.1406	Class2		
21.8366	3599.8582	9.4154	8.1406	10.6902	Class3		
55.2370	9106.0589	17.1586	10.6902	23.6270	Class4		
8.8314	1455.8984	0.6802	0.4129	0.9475	Class1	2021_1_17	
29.4672	4857.7960	1.5592	0.9475	2.1708	Class2		
38.2902	6312.3093	2.7213	2.1708	3.2718	Class3		
23.4112	3859.4381	7.3698	3.2718	11.4679	Class4		
14.0541	2316.8853	5.4601	4.2459	6.6742	Class1	2021_7_18	
32.4784	5354.2030	7.2702	6.6742	7.8663	Class2		
53.4601	8813.1386	8.4844	7.8663	9.1025	Class3		
0.0074	1.2150	12.3034	9.1025	15.5043	Class4		
100	16485.4418	Total					

### Conclusions:-

1- The possibility of calculating evapotranspiration (mm) using digital modeling for remote sensing and geographic information systems.

2- The proposed model proved accurate in calculating the values of evapotranspiration (mm) in the study area, completely that dependent on the fourth, fifth, and tenth spectral bands.

3- The values of evapotranspiration can be calculated for large areas and remote areas that are difficult to reach its by using the proposed model.

4- The values of evapotranspiration increased in areas with bare soils in July compared to moist soils in January.

5- The vegetation cover has a great impact on the values of evapotranspiration, as the rates of evapotranspiration increase as the

vegetation cover decreases and vice versa due to the positive effect of the vegetation cover on lowering temperatures and covering the soil surface.

6- Basra Governorate suffers from a rise in the values of evapotranspiration from some limited areas due to the presence of oil fields , the burning of natural gas, and some electric power plants.

## References

- Farina, F. (2012).** Exploring the relationship between land surface temperature and vegetation abundance for urban heat island mitigation in Seville, Spain. Department of Earth and Ecosystem Sciences, Division of Physical Geography and Ecosystem Analysis , Centre for Geographical Information Systems , Lund University Sölvegatan 12 . LUMA-GIS Thesis nr 15.
- Haimed, Mohamed Majid (2019):** Using remote sensing data and the SEBAL algorithm to study the temporal variability in temperature and soil moisture in the Al-Musayyab project. Master's thesis - College of Agricultural Engineering Sciences - University of Baghdad.
- Gontia N. K and Tiwari, K. N. (2010).** Estimation of crop coefficient and evapotranspiration of wheat (*Triticum aestivum*) in an irrigation command using remote sensing and GIS. *Water Resources Management*. vol. 24. no. 7, pp. 1399–1414.
- González, Arturo Reyes . Jeppe Kjaersgaard, Todd Trooien, Christopher Hay, and Laurent Ahiablame (2018).** Estimation of Crop Evapotranspiration Using Satellite Remote Sensing-Based Vegetation Index. *Advances in Meteorology*. <https://doi.org/10.1155/2018/4525021>.
- Howari, F. M., Manish Sharma, Cijo M Xaviera, Yousef Nazzala, Imen Ben Salema, and Fatima AlAydarosb ,H. (2022).** Remote sensing and GIS based approaches to estimate evapotranspiration in the arid and semi- arid regions. *Remote Sensing for Agriculture, Ecosystems and Hydrology*, 1, 11856- 11021.
- Howari, F. M., Murad, A., & Garamoon, H. (2006).** Prediction of spatial ET-fluxes using remote sensing and field data of selected areas in the Eastern Part of Abu Dhabi, United Arab Emirates. *Soil Research*, 44(8), 759-768.
- Lal R. , and M. K. Shukla ( 2004).** Principles of Soil Physics. The Ohio State University Columbus, Ohio, U.S.A.
- Moorhead, J. E. , G.W. Marek , P. D. Colaizzi , P. H. Gowda , S. R. Evett , D. K. Brauer , T. H. Marek and D. O. Porter . (2017).** Evaluation of Sensible Heat Flux and Evapotranspiration Estimates Using a Surface Layer Scintillometer and a Large Weighing Lysimeter. *Sensors*, 17, 2350; doi:10.3390/s17102350.
- Onwuka B. and B. Mang (2018).** Effects of Soil Temperature on Some Soil Properties and Plant Growth. Department of Soil Science and Meteorology, Michael Okpara University of Agriculture, Nigeria. *Advances Plants and Agriculture Research* 8(1) : 00288. DOI:

